catalysts

MDPI

Article

Vanadium Oxide Supported on MSU-1 as a Highly Active Catalyst for Dehydrogenation of Isobutane with CO_2

Guosong Sun [1,2,*], Qingze Huang [2], Shiyong Huang [2], Qiuping Wang [2], Huiquan Li [3], Haitao Liu [3], Shijie Wan [4], Xuewang Zhang [2] and Jinshu Wang [1,*]

1 The College of Materials Science and Engineering, Beijing University of Technology, Beijing 100022, China
2 Guangxi Research Institute of Chemical Industry, Nanning 530001, China; huang0823@126.com (Q.H.); shiyonghuang@163.com (S.H.); wangqiuping8287@163.com (Q.W.); zxw507@163.com (X.Z.)
3 Key Laboratory for Green Process and Engineering, Institute of Process Engineering, Chinese Academy of Sciences, Beijing 100190, China; hqli@home.ipe.ac.cn (H.L.); liuht@home.ipe.ac.cn (H.L.)
4 Guangxi Branch of China Academy of Science & Technology Development, Nanning 530001, China; wanshijie01@126.com
* Correspondence: sungsgx@163.com (G.S.); wangjsh@bjut.edu.cn (J.W.); Tel.: +86-77-1330-6235 (G.S.); +86-10-6739-1101 (J.W.); Fax: +86-77-1331-5527 (G.S.); +86-10-6739-1101 (J.W.)

Academic Editor: Michalis Konsolakis
Received: 12 January 2016; Accepted: 7 March 2016; Published: 9 March 2016

Abstract: Vanadium oxide supported on MSU-1, with VO_x loading ranging from 2.5 to 17.5 wt. %, was developed as a highly active catalyst in dehydrogenation of isobutane with CO_2. The obtained catalysts of VO_x/MSU-1 were characterized by X-ray diffraction (XRD), N_2 adsorption-desorption, and H_2-temperature programmed reduction (H_2-TPR) methods and the results showed that the large surface area of MSU-1 was favorable for the dispersion of VO_x species and the optimal loading of VO_x was 12.0 wt. %. Meanwhile, the catalytic activity of VO_x/MSU-1 was investigated, and VO_x/MSU-1 with 12.0 wt. % VO_x content was found to be the best one, with the conversion of isobutane (58.8%) and the selectivity of isobutene (78.5%) under the optimal reaction conditions. In contrast with the reaction in the absence of CO_2, the presence of CO_2 in the reaction stream could obviously enhance the isobutane dehydrogenation, which raised the conversion of reaction and the stability of VO_x/MSU-1.

Keywords: VO_x/MSU-1 catalyst; isobutane; dehydrogenation; isobutene; CO_2

1. Introduction

Dehydrogenation of lower alkanes to alkenes is always attractive research around the world [1–4]. With the use of downstream products of isobutene increasing [5,6], the demand of isobutene is rapidly growing, so the dehydrogenation of isobutane to isobutene is becoming one of the important ways to produce isobutene. The process of dehydrogenation can be classified into two types: direct dehydrogenation and oxidative dehydrogenation. In fact, the direct dehydrogenation of isobutane to isobutene has been achieved in industrialization [7], but there are still some serious technical problems, such as high production cost, complex processing, and deactivation of the catalyst by carbon deposition. As a result, the oxidative dehydrogenation of isobutane (ODB) has received more and more attention, recently [8,9]. ODB will not be limited by thermodynamic equilibrium, so the conversion of isobutane can obviously be raised and the energy consumption can be greatly reduced. Due to the deep oxidation of product, there is lower isobutene selectivity using oxygen (O_2) as an oxidant [10,11]. Recently, CO_2 has received much attention as a co-feed gas for dehydrogenation, because CO_2 can act as a mild oxidant [12–15]. Unlike oxygen, CO_2 will not be able to fully oxidize the catalyst to its original state due to its weak oxidation capacity. It is a thermodynamically stable and a kinetically inert molecule,

and it is also cheap and abundant. Moreover, because of its high heat capacity, using CO_2 as a co-feed can alleviate the effects of the exothermal ODB reaction, avoiding hot spots that can lead to cracking of the alkane [14,16]. It has been confirmed that CO_2 had the ability to partially refresh active species on the catalysts and participated in the oxidative dehydrogenation [17]. When CO_2 was present in the feed, the reaction followed the oxidative dehydrogenation route but was also accompanied by the reverse water gas shift (RWGS) reaction in combination with the direct dehydrogenation route [17,18]. Moreover, CO_2 can eliminate coke deposited over the catalysts, to some extent, and improve the stability of catalysts [19]. Therefore, in recent years, the research of dehydrogenation of isobutane with CO_2 has been actively studied, which mainly focused on the development of different catalysts.

The catalysts containing vanadium were found to have excellent catalytic activity for the dehydrogenation reaction [20–25]. Ogonowski *et al.* [24] loaded vanadium oxides on active carbon (AC), SiO_2, Al_2O_3, and ZnO, and found that the key factor influencing catalytic activity was the alkalinity/acidity of catalyst surface and oxidation-reduction potential of vanadium species. Research of Ma *et al.* [25] on V_2O_5/Al_2O_3 and V_2O_5/SiO_2 catalyst showed that vanadium species with higher dispersion had better catalytic activity. However, the traditional carriers, such as Al_2O_3 and SiO_2, possessed low specific surface area, small pore size and wide pore size distribution, which restricted the activity of catalysts. In view of these, mesoporous materials used as the carrier were widely studied. MSU-*x* is an important family of mesoporous material, with 3D worm-like holes, which possess many advantages of pore structure and is in favor of the diffusion of molecular objects [26]. Furthermore, the non-ionic surfactants used as templates in the synthesis of MSU-*x* materials are low-cost, non-toxic, and biodegradable; thus, it is more suitable for the carriers of catalysts. In the early work of our group, the catalysts had been prepared by loading chromium on MSU-*x* for catalytic dehydrogenation of propane and ethane [27–30], which had showed high catalytic activity.

In this paper, MSU-1, was prepared at room temperature using sodium silicate as the source of silicon. Then, vanadium oxide, VO_x, was loaded over the carrier of MSU-1 and a series of vanadium-based catalysts, VO_x/MSU-1, were prepared by wet impregnation method. The obtained catalysts were characterized with X-ray diffraction (XRD), N_2 adsorption-desorption, and H_2-temperature programmed reduction (H_2-TPR) techniques. The catalytic performance of VO_x/MSU-1 was investigated for the dehydrogenation of isobutane with or without CO_2.

2. Results and Discussion

2.1. Catalyst Characterization

Figure 1 showed XRD patterns of the samples prepared, including undoped and VO_x-modified MSU-1 (VO_x/MSU-1) in two different regions of 2θ angle, where they were 0.5°–10° and 10°–85°. In the 2θ range of 0.5°–10°, one well-resolved diffraction peak was observed (Figure 1A), which corresponded to d_{100} reflection [31]. This result clearly indicated that they all had the typically less long-range-ordered, worm-like mesoporous structure. Compared with undoped MSU-1, the intensity of diffraction peak of VO_x-containing MSU-1 gradually decreased with VO_x content increasing. However, even in the case of MSU-1 with the highest VO_x loading, 17.5 wt. %, the d_{100} diffraction peak were still obviously observed, indicating that the mesoporous structure of the catalysts, VO_x/MSU-1, remained well during impregnation and subsequent calcination.

According to the large-angle XRD patterns of 10°–85° (Figure 1B), it could be seen that the diffraction peaks corresponding to crystal phase of V_2O_5 were 15.5°, 20.2°, 26.2°, and 31.1°. However, these peaks were absent for the samples with VO_x loading lower than 12.0 wt. %. This could be attributed to high dispersion of crystal phase of bulk V_2O_5 on the surface of MSU-1. When VO_x loading reached 17.5 wt. %, the peaks became very clear, which indicated that more and larger crystal phase of bulk V_2O_5 appeared over MSU-1 with the increase of VO_x loading. The catalytic activity and selectivity of vanadium oxide for oxidative dehydrogenation depended on its structure, dispersion, and the characteristics of its supporting material. The most active catalytic form for this type of reaction

was the monomeric, isolated VO_x species [32]. The presence of bulk V_2O_5 on the other hand decreased the selectivity and favored total oxidation. So, the fit VO_x loading for VO_x/MSU-1 catalysts should be 12.0 wt. % or so.

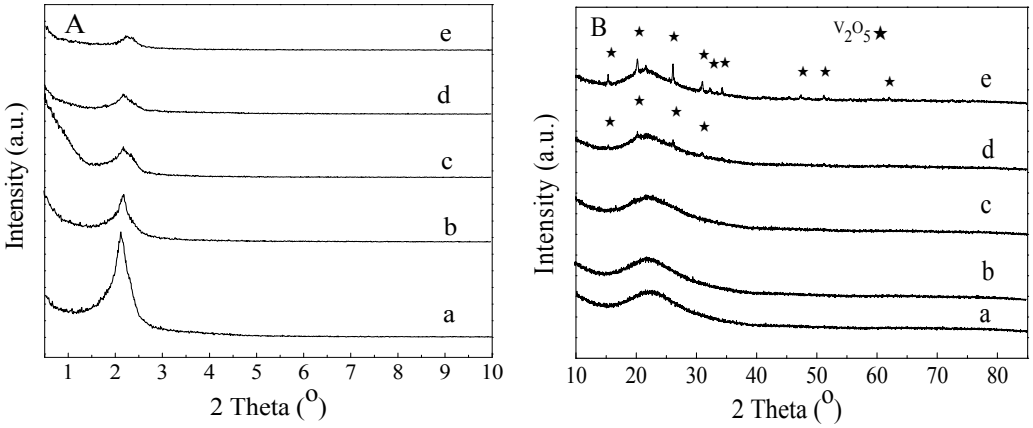

Figure 1. X-ray diffraction (XRD) patterns of MSU-1 and VO_x/MSU-1 with different VO_x loading. (**A**) 2θ in the range of 0.5°–10°; (**B**) 2θ in the range of 10°–85°. (**a**) MSU-1; (**b**) 2.5 wt. % VO_x/MSU-1; (**c**) 7.0 wt. % VO_x/MSU-1; (**d**) 12.0 wt. % VO_x/MSU-1; and (**e**) 17.5 wt. % VO_x/MSU-1.

Table 1 listed Brunauer-Emmett-Teller (BET) surface area and pore volume of undoped and VO_x-modified MSU-1. From Table 1, it could be seen that the carrier of MSU-1 possessed high-surface area (1021.3 m^2/g) and moderate pore volume (0.54 cm^3/g), which was favorable for the dispersion of active components. As for VO_x/MSU-1 samples, both surface area and pore volume decreased gradually with VO_x content increasing in comparison to MSU-1. This could be due to that more VO_x loading led to the formation of larger VO_x crystals and as a result, a certain amount of MSU-1 pores was blocked by the bulk crystals, which was also confirmed by XRD patterns of VO_x/MSU-1 samples (Figure 1). When VO_x loading was 17.5 wt. %, the surface area and pore volume of VO_x/MSU-1 decreased to 297.9 m^2/g and 0.30 cm^3/g, respectively, which was not advantageous to the dehydrogenation of isobutane.

Table 1. Physical properties of MSU-1 and VO_x/MSU-1 with different VO_x loading.

Samples	BET Surface Area (m^2/g)	Pore Volume (cm^3/g)
MSU-1	1021.3	0.54
2.5 wt. % VO_x/MSU-1	748.4	0.40
7.0 wt. % VO_x/MSU-1	655.7	0.33
12.0 wt. % VO_x/MSU-1	539.4	0.34
17.5 wt. % VO_x/MSU-1	297.9	0.30

The pore diameter distribution of different samples was shown in Figure 2, which was determined by Barrett-Joyner-Halenda (BJH) method. As shown in Figure 2, the peak at 2.2 nm was attributed to the characteristic behavior of mesoporous materials MSU-1, and the pore size distribution was narrow and normal, indicating that the carrier of MSU-1 had a uniform pore structure. Moreover, with VO_x content increasing, the peak shape gradually moved to the left, as a whole, and the width of peak also increased in the meantime. When VO_x loading reached 17.5 wt. %, the peak had moved to 1.8 nm from 2.2 nm, which suggested that some pores of MSU-1 might be partly occupied by vanadium oxides, resulting in smaller pore size. As a result, the pore size distribution of VO_x/MSU-1 catalysts were broadened and the surface area and pore volume were decreased.

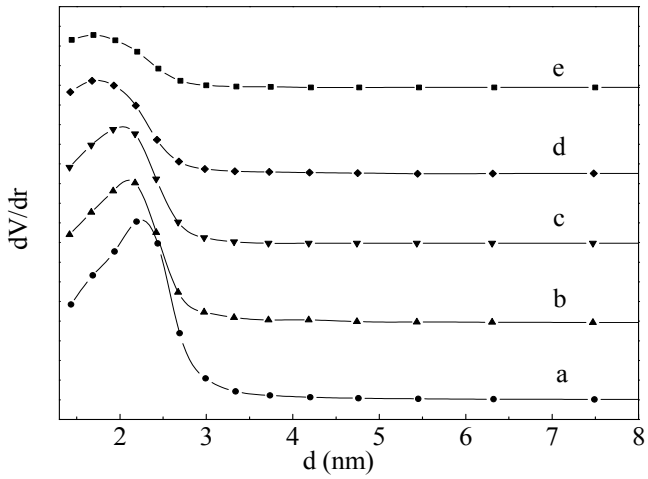

Figure 2. Pore diameter distribution of MSU-1 and VO_x/MSU-1 with different VO_x loading. (**a**) MSU-1; (**b**) 2.5 wt. % VO_x/MSU-1; (**c**) 7.0 wt. % VO_x/MSU-1; (**d**) 12.0 wt. % VO_x/MSU-1; and (**e**) 17.5 VO_x/MSU-1.

H_2-TPR patterns of undoped MSU-1 and VO_x/MSU-1 catalysts with different VO_x loading were comparatively shown in Figure 3. There were no H_2 consumption peaks to be found for undoped MSU-1 in Figure 3. For the samples containing 2.5–12.0 wt. % VO_x, a weak reduction peak at 680–720 K were observed, in which vanadium species existed mainly in the form of surface oligo-species with the octahedral coordination [33]. TPR curves of all VO_x-supported samples, VO_x loading from 2.5 wt. % to 17.0 wt. %, exhibited one strong reduction peak in the temperature range of 820–850 K, which was found to shift to higher temperatures as the VO_x loading was increased, suggesting increased particle size of microcrystalline vanadia with loading. This has been confirmed that as the vanadia species became more bulk-like, *i.e.*, the particle size increased with an increase in loading, the vanadia became more difficult to reduce due to bulk diffusion limitations resulting in a shift in TPR peaks to higher temperatures [33,34]. The samples, containing more than 7.0 wt. % VO_x were characterized by new peaks appearing already between 920 and 970 K, which gradually increased with VO_x loading, showing that more bulk-like VO_x crystals had been shaped. This had been concluded that there was a correlation between the reducibility of surface vanadium species and their catalytic properties. High activity was ascribed to vanadate species, either isolated or polymerized up to the formation of a VO_x monolayer, whereas lower activity was usually associated with the presence of bulk V_2O_5 [34,35].

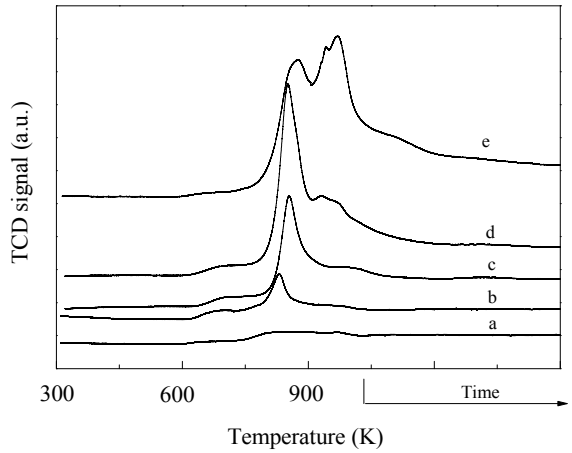

Figure 3. H_2-temperature programmed reduction (H_2-TPR) profiles of MSU-1 and VO_x/MSU-1 with different VO_x loading. (**a**) MSU-1; (**b**) 2.5 wt. % VO_x/MSU-1; (**c**) 7.0 wt. % VO_x/MSU-1; (**d**) 12.0 wt. % VO_x/MSU-1; and (**e**) 17.5 wt. % VO_x/MSU-1.

2.2. Catalytic Performance

The catalytic performance of VO_x/MSU-1 with different VO_x loading for the isobutane dehydrogenation were shown in Table 2, where the main byproducts of reaction were also listed out, including propylene (C_3H_6) and methane (CH_4). Undoped MSU-1 exhibited low catalytic activity in comparison to VO_x-doped samples, with 11.8% conversion of isobutane (i-C_4H_{10}) and 52.5% selectivity of isobutene (i-C_4H_8) (Entry 1). The conversion of isobutane gradually increased with VO_x loading, and reached maximum value, 58.8% (Entry 4), when VO_x loading was 12 wt. %. While VO_x loading further increased to 17.5 wt. %, the conversion of isobutane begun to decrease to 51.0% (Entry 6). This could be due to that more VO_x loading resulted in the poor dispersion of VO_x species and formation of more bulk-like VO_x crystals, which had been demonstrated by XRD (Figure 1) and H_2-TPR (Figure 3) characterization. However, the selectivity of isobutene did not exhibit obvious change in a certain extent with the increase of VO_x loading, basically keeping at 79% or so. The selectivity of main byproducts, propylene and methane, also remained stable in principle, approximately 10% and 5%, respectively. Moreover, contrasting Entries 4 and 5 in Table 2, it could be found that the presence of CO_2 significantly enhanced the efficiency of isobutane dehydrogenation, which was generally attributed to that CO_2 as a weak oxidant could eliminate hydrogen produced during the dehydrogenation through RWGS reaction [18,36]. Coupling of RWGS reaction with the dehydrogenation reaction therefore improved the equilibrium conversion of reaction toward isobutene production. In Table 2, with CO_2 conversion increasing, the conversion of isobutane gradually increased, which further confirmed the role of CO_2 coupling reaction.

Table 2. Catalytic performance for isobutane dehydrogenation over VO_x/MSU-1 with different VO_x loading.

Entry	VO_x Loading (wt. %)	Conversion (%)		Selectivity (%)			Yield (%)
		i-C_4H_{10}	CO_2	i-C_4H_8	C_3H_6	CH_4	i-C_4H_8
1	0	11.8	0.6	52.5	30.2	13.6	6.2
2	2.5	36.3	7.7	79.5	9.6	4.6	28.9
3	7.0	54.9	14.8	79.2	9.4	4.7	43.5
4	12.0	58.8	16.9	78.5	9.9	5.4	46.2
5	12.0*	40.5	/	82.8	10.5	6.6	33.5
6	17.5	51.0	15.2	78.9	9.8	5.6	40.2

Reaction conditions: reaction temperature 873 K, total flow rate 24 mL/min, catalyst 0.2 g, V(CO_2):V(i-C_4H_{10}) = 3:1; * V(Ar):V(i-C_4H_{10}) = 3:1.

The effect of temperature on the dehydrogenation of isobutane with CO_2 were shown in Figure 4, using 12 wt. % VO_x/MSU-1 as catalyst. The conversion of isobutane gradually increased as the reaction temperature was raised, whereas the selectivity of isobutene, the object product, decreased on the contrary. Although high temperature could accelerate the dehydrogenation rate of isobutane, meanwhile the elevation of temperature favored cracking of isobutane to produce propylene and methane. So, considering all reaction factors, 873 K was chosen as the optimal reaction temperature, with the conversion of isobutane 58.8% and the selectivity of isobutene 78.5%.

Figure 5 exhibited the catalytic activity of 12 wt. % VO_x/MSU-1 as a function of reaction time. As the reaction proceeded, the isobutane conversion of dehydrogenation gave a visible drop, either in the presence of or in the absence of CO_2, suggesting that the catalyst was deactivated to some degree. In contrast with the reaction in the absence of CO_2, the presence of CO_2 in the reaction stream here could obviously enhance the stability of VO_x/MSU-1, and the drop rate of isobutane conversion with CO_2 was lower than that without CO_2. For example, the conversion of isobutane decreased from primal 58.8% to 44.2% with CO_2 and 40.5% to 21.9% without CO_2, respectively, after reacting for 3 h. This was due to that CO_2 in the reaction stream could suppress the formation of coke deposited over VO_x/MSU-1 [17,37,38]. Moreover, from Figure 5, it could also be seen that the selectivity to isobutene gave a slight increase with proceeding reaction, especially with CO_2.

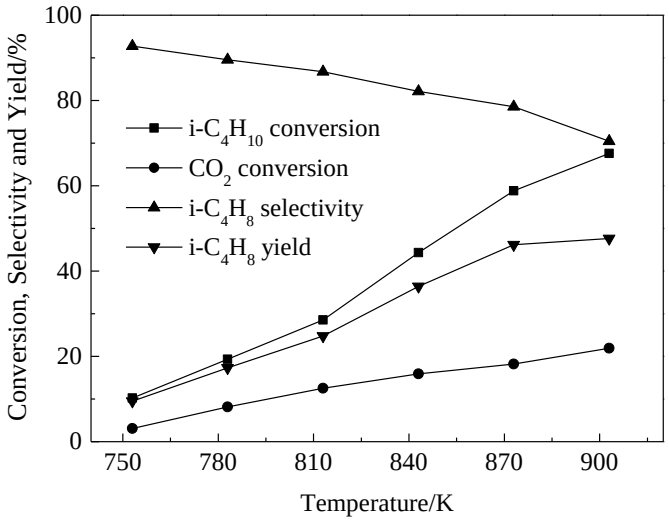

Figure 4. Effect of temperature on dehydrogenation of isobutane to isobutene with CO_2 over VO_x/MSU-1. Reaction conditions: 12 wt. % VO_x/MSU-1 0.2 g; total flow rate 24 mL/min; V(CO_2):V(*i*-C_4H_{10}) = 3:1.

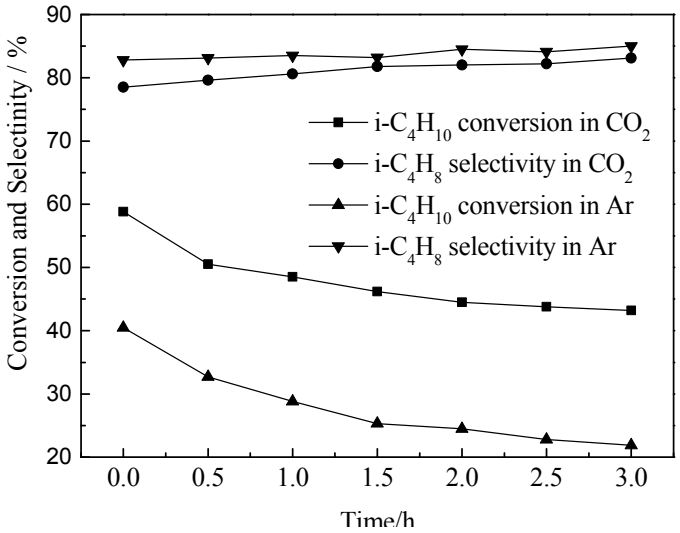

Figure 5. Catalytic stability in dehydrogenation of isobutane to isobutene with CO_2 or Ar over VO_x/MSU-1. Reaction conditions: reaction temperature 873 K, total flow rate 24 mL/min, 12 wt. % VO_x/MSU-1 0.2 g, V(CO_2):V(*i*-C_4H_{10}) = 3:1 or V(Ar):V(*i*-C_4H_{10}) = 3:1.

3. Experimental Section

3.1. Catalyst Preparation

The carrier of MSU-1 was prepared at room temperature using sodium silicate as the source of silicon by the method reported before [22,23]. All the catalysts of VO_x/MSU-1 were prepared by wet impregnation method. Typically, 2 g of dry MSU-1 was treated with 20 mL of aqueous solution containing the desired amount of NH_4VO_3 (analytically pure) overnight. The impregnated samples were evaporated and dried at 353 K for 7 h and finally calcined under air at 873 K for 4 h. These catalysts are designated as *x* wt. % VO_x/MSU-1, where *x* expresses the total VO_x loading.

3.2. Catalyst Characterization

XRD patterns were recorded in two ranges of 0.5°–10.0° and 10°–85° (2θ) at room temperature, using X'pert Pro MPD X-ray diffractometer from PANalytical (Almelo, Holland) operated at 40 kV and 30 mA, equipped with a Cu $K\alpha$ X-ray source.

N_2 adsorption-desorption measurements were carried out on an Autosorb series ASIMP apparatus from Quantachrome (Boynton Beach, FL, USA). Before measurements, the samples were degassed at 573 K under vacuum for 3 h. Calculation of specific surface area (BET), pore volume and pore size distribution (BJH method) were performed with the software of the apparatus.

H_2-TPR analysis (self-made experimental instrument) were performed using Ar/H_2 gas mixture (95/5 vol %). The total flow rate of the feed was 30 mL/min. Before experiment the sample (100 mg) was preheated in a stream of dry argon at 873 K for 30 min, and then cooled to room temperature. The samples were heated at 15 K/min to the final temperature of 1073 K. H_2 consumption was measured by a thermal conductivity detector and V_2O_5 was used as a reference for the calibration of H_2 consumption.

3.3. Catalytic Tests

The catalytic tests of isobutane dehydrogenation were carried out in a fixed-bed quartz tubular reactor with an inner diameter of 6.0 mm at 773–973 K and atmospheric pressure. For each test, about 0.2 g of catalyst sample (40–60 mesh) was diluted with quartz grain and loaded in the constant temperature zone of the reactor. The reaction stream was constituted of isobutane and CO_2 or Ar with the mole ratio of $n(CO_2)/n(C_4H_{10})$ or $n(Ar)/n(C_4H_{10})$ being 3 and the total flow rate being 24 mL/min.

The reactants and products were analyzed on-line using a gas chromatograph (Shimadzu GC-2014, Kyoto, Japan). One of column was equipped Rt-Al_2O_3 (30 m × 0.53 mm × 10.0 μm) and a flame ionization detector. This column was used to analyze hydrocarbons C_1–C_4. The second column was equipped GDX-502 (3 m × 2 mm) and a thermal conductivity detector for CO and CO_2 analyses, which carrier gas is He. Conversion (C) of isobutane and carbon dioxide and selectivity (S) of isobutene and other byproducts were calculated according to the following equations:

$$C_{C_4H_{10}} = \frac{n_{C_4H_8} + \frac{3}{4}n_{C_3H_8} + \frac{3}{4}n_{C_3H_6} + \frac{1}{2}n_{C_2H_6} + \frac{1}{2}n_{C_2H_4} + \frac{1}{4}n_{CH_4}}{n_{C_4H_{10}} + n_{C_4H_8} + \frac{3}{4}n_{C_3H_8} + \frac{3}{4}n_{C_3H_6} + \frac{1}{2}n_{C_2H_6} + \frac{1}{2}n_{C_2H_4} + \frac{1}{4}n_{CH_4}} \times 100\% \quad (1)$$

$$C_{CO_2} = \frac{n_{CO}}{n_{CO} + n_{CO_2}} \times 100\% \quad (2)$$

$$S_i = \frac{\frac{a_i}{4}n_i}{n_{C_4H_8} + \frac{3}{4}n_{C_3H_8} + \frac{3}{4}n_{C_3H_6} + \frac{1}{2}n_{C_2H_6} + \frac{1}{2}n_{C_2H_4} + \frac{1}{4}n_{CH_4}} \times 100\% \quad (3)$$

where a_i was the number of carbon atoms of the compound i and n_i is the mole number of the compound i. The calculations did not consider the conversion of isobutane to coke.

4. Conclusions

In conclusion, the catalysts of VO_x/MSU-1, prepared by loading VO_x over MSU-1, were active and selective in the oxidative dehydrogenation of isobutane with CO_2. Their catalytic properties were related to the VO_x loading and high surface area of MSU-1. XRD, N_2 adsorption-desorption and H_2-TPR characterization for VO_x/MSU-1 showed that the optimal loading of VO_x was 12.0 wt. % and more VO_x could led to the formation of larger bulk-like VO_x crystals and the decrease of the surface area and pore volume. As a result, 12.0 wt. % VO_x/MSU-1 exhibited the highest catalytic activity, with the conversion of isobutane 58.8% and the selectivity of isobutene 78.5% at 873 K. In the feed of reactants, the presence of CO_2 played quite important role on the dehydrogenation of isobutane,

which not only could remove H_2 produced in the reaction through RWGS reaction but also suppress the formation of coke deposits and improve the stability of VO_x/MSU-1.

Acknowledgments: This work was supported by grants from the National Natural Science Foundation of China (No. 21006109) and the Guangxi Science Foundation of China (2012GXNSFBA053033 & 2011GXNSFA018053).

Author Contributions: Guosong Sun and Jinshu Wang conceived and designed the experiments; Guosong Sun, Qingzhe Huang and Qiuping Wang performed the experiments; Shiyong Huang, Haitao Liu and Huiquan Li contributed to data analysis and discussion; Guosong Sun, Qingzhe Huang, Shiyong Huang and Jishu Wang wrote and revised the manuscript; Shijie Wan was responsible for supplementing the detailed role of CO_2 during the reaction in the introduction; Xuewang Zhang contributed to the supplementary explanation of X-ray diffraction (XRD), H_2-temperature programmed reduction (H_2-TPR) and other experimental data.

Conflicts of Interest: The authors declare no conflict of interest.

References

1. Wang, S.B.; Murata, K.; Hayakawa, T.; Hamakawa, S.; Suzuki, K. Dehydrogenation of ethane with carbon dioxide over supported chromium oxide catalysts. *Appl. Catal. A* **2000**, *196*, 1–8. [CrossRef]
2. Tasbihi, M.; Feyzi, F.; Amlashi, M.A.; Abdullah, A.Z.; Mohamed, A.R. Effect of the addition of potassium and lithium in Pt-Sn/Al_2O_3 catalysts for the dehydrogenation of isobutane. *Fuel Process. Technol.* **2007**, *88*, 883–889. [CrossRef]
3. Wang, M.G.; Zhong, S.H. Pd/V_2O_5-SiO_2 catalyst for oxidative dehydrogenation of isobutane with CO_2 to isobutene. *Chin. J. Catal.* **2007**, *28*, 124–130.
4. Rombi, E.; Gazzoli, D.; Cutrufello, M.G.; De Rossi, S.; Ferino, I. Modifications induced by potassium addition on chromia/alumina catalysts and their influence on the catalytic activity for the oxidative dehydrogenation of propane. *Appl. Surf. Sci.* **2010**, *256*, 5576–5580. [CrossRef]
5. Seddon, D. Reformulated gasoline, opportunities for new catalyst technology. *Catal. Today* **1992**, *15*, 1–21. [CrossRef]
6. Iannazzo, V.; Neri, G.; Galvagno, S.; Di Serio, M.; Tesser, R.; Santacesaria, E. Oxidative dehydrogenation of isobutane over V_2O_5-based catalysts prepared by grafting vanadyl alkoxides on TiO_2-SiO_2 supports. *Appl. Catal. A* **2003**, *246*, 49–68. [CrossRef]
7. Resasco, D.E.; Marcus, B.K.; Huang, C.S.; Durante, V.A. Isobutane dehydrogenation over sulfided nickel catalysts. *J. Catal.* **1994**, *146*, 40–55. [CrossRef]
8. De Rossi, S.; Ferraris, G.; Fremiotti, S.; Indovina, V.; Cimino, A. Isobutane dehydrogenation on chromia/zirconia catalysts. *Appl. Catal. A* **1993**, *106*, 125–141. [CrossRef]
9. Gniot, I.; Kirszensztejn, P.; Kozlowski, M. Oxidative dehydrogenation of isobutane using modified activated carbons as catalysts. *Appl. Catal. A* **2009**, *362*, 67–74. [CrossRef]
10. Zhang, L.; Deng, J.; Dai, H.; Au, C.T. Binary Cr-Mo oxide catalysts supported on MgO-coated polyhedral three-dimensional mesoporous SBA-16 for the oxidative dehydrogenation of iso-butane. *Appl. Catal. A* **2009**, *354*, 72–81. [CrossRef]
11. Neri, G.; Pistone, A.; De Rossi, S.; Rombi, E.; Milone, C.; Galvagno, S. Ca-doped chromium oxide catalysts supported on alumina for the oxidative dehydrogenation of isobutane. *Appl. Catal. A* **2004**, *260*, 75–86. [CrossRef]
12. Castro, A.J.R.; Soares, J.M.; Filho, J.M.; Oliveira, A.C.; Campos, A.; Milet, É.R.C. Oxidative dehydrogenation of ethylbenzene with CO_2 for styrene production over porous iron-based catalysts. *Fuel* **2013**, *108*, 740–748. [CrossRef]
13. Chen, S.W.; Qin, Z.F.; Wang, G.F.; Dong, M.; Wang, J.G. Promoting effect of carbon dioxide on the dehydrogenation of ethylbenzene over silica-supported vanadium catalysts. *Fuel* **2013**, *109*, 43–48. [CrossRef]
14. Wu, R.; Xie, P.; Cheng, Y.; Yue, Y.; Gu, S.; Yang, W.; Miao, C.; Hua, W.; Gao, Z. Hydrothermally prepared Cr_2O_3–ZrO_2 as a novel efficient catalyst for dehydrogenation of propane with CO_2. *Catal. Commun.* **2013**, *39*, 20–23. [CrossRef]
15. Wang, S.; Zhu, Z.H. Catalytic conversion of alkanes to olefins by carbon dioxide oxidative dehydrogenation-a review. *Energy Fuels* **2004**, *18*, 1126–1139. [CrossRef]

16. Ajayi, B.P.; Jermy, B.R.; Ogunronbi, K.E.; Abussaud, B.A.; Al-Khattaf, S. *n*-Butane dehydrogenation over mono and bimetallic MCM-41 catalysts under oxygen free atmosphere. *Catal. Today* **2013**, *204*, 189–196. [CrossRef]
17. Ascoop, I.; Galvita, V.V.; Alexopoulos, K.; Reyniers, M.; Van Der Voort, P.; Bliznuk c, V.; Marin, G.B. The role of CO_2 in the dehydrogenation of propane over WO_x-VO_x/SiO_2. *J. Catal.* **2016**, *335*, 1–10.
18. Ding, J.F.; Qin, Z.F.; Li, X.K.; Wang, G.F.; Wang, J.G. Catalytic dehydrogenation of isobutane in the presence of carbon dioxide over nickel supported on active carbon. *J. Mol. Catal. A* **2010**, *315*, 221–225. [CrossRef]
19. Ogonowski, J.; Skrzyńska, K. Carbon dioxide in the dehydrogenation of isobutane over $VMgO_x$. *Catal. Commun.* **2009**, *11*, 132–136. [CrossRef]
20. Carrazán, S.R.G.; Peres, C.; Bernard, J.P.; Ruwet, M.; Ruiz, P.; Delmon, B. Catalytic synergy in the oxidative dehydrogenation of propane over MgVO catalysts. *J. Catal.* **1996**, *158*, 452–476. [CrossRef]
21. Takita, Y.; Xia, Q.; Kikutani, K.; Soda, K.; Takami, H.; Nishigushi, H.; Nagaoka, K. Anaerobic oxidation of isobutane: II. Catalysis by Mg-V complex oxides. *J. Mol. Catal. A* **2006**, *248*, 61–69. [CrossRef]
22. Fu, Y.; Ma, H.; Wang, Z.; Zhu, W.; Wu, T.; Wang, G. Characterization and reactivity of SnO_2-doped V_2O_5/γ-Al_2O_3 catalysts in dehydrogenation of isobutane to isobutene. *J. Mol. Catal. A* **2004**, *221*, 163–168. [CrossRef]
23. Ogonowski, J.; Skrzyńska, E. Deactivation of $VMgO_x$ catalysts by coke in the process of isobutane dehydrogenation with carbon dioxide. *Catal. Lett.* **2008**, *121*, 234–240. [CrossRef]
24. Ogonowski, J.; Skrzyńska, E. Activity of vanadium magnesium oxide supported catalysts in the dehydrogenation of isobutane. *Catal. Lett.* **2006**, *111*, 79–85. [CrossRef]
25. Ma, H.; Liu, Z.; Wang, Z.; Zhu, W.; Wang, G. Study of V_2O_5/γ-Al_2O_3 catalyst for dehydrogenation of isobutane. *Chin. J. Appl. Chem.* **2002**, *19*, 290–294.
26. Prouzet, É.; Boissière, C. A review on the synthesis, structure and applications in separation processes of mesoporous MSU-*x* silica obtained with the two-step process. *Comptes Rendus Chim.* **2005**, *8*, 579–596. [CrossRef]
27. Liu, L.; Li, H.; Zhang, Y. A comparative study on catalytic performances of chromium incorporated and supported mesoporous MSU-*x* catalysts for theoxidehydrogenation of ethane to ethylene with carbon dioxide. *Catal. Today* **2006**, *115*, 235–241. [CrossRef]
28. Liu, L.; Li, H.; Zhang, Y. Mesoporous silica-supported chromium catalyst: Characterization and excellent performance in dehydrogenation of propaneto propylene with carbon dioxide. *Catal. Comm.* **2007**, *8*, 565–570. [CrossRef]
29. Liu, H.; Li, H.; Yang, W.; Wang, X.; Zhang, Y. Effect of Cr content on catalytic performance of Cr/MSU-1 catalysts in oxidative dehydrogenation of propane to propylene with CO_2. *Acta Chim. Sin.* **2009**, *15*, 1749–1753.
30. Liu, L.; Li, H.; Zhang, Y. Effect of synthesis parameters on the chromium content and catalytic activities of mesoporous Cr-MSU-*x* prepared under acidic conditions. *J. Phys. Chem. B* **2006**, *110*, 15478–15485. [CrossRef] [PubMed]
31. Sierra, L.; Guth, J.L. Synthesis of mesoporous silica with tunable pore size from sodium silicate solutions and a polyethylene oxide surfactant. *Micropor. Mesopor. Mater.* **1999**, *27*, 243–253. [CrossRef]
32. Rossetti, I.; Fabbrini, L.; Ballarini, N.; Oliva, C.; Cavani, F.; Cericola, A.; Bonelli, B.; Piumetti, M.; Garrone, E.; Dyrbeck, H.; *et al*. V_2O_5-SiO_2 systems prepared by flame pyrolysis as catalysts for the oxidative dehydrogenation of propane. *J. Catal.* **2008**, *256*, 45–61. [CrossRef]
33. Koranne, M.M.; Goodwin, J.G.; Marcelin, G. Characterization of silica- and alumina-supported vanadia catalysts using temperature programmed reduction. *J. Catal.* **1994**, *148*, 369–377. [CrossRef]
34. Adamski, A.; Sojka, Z.; Dyrek, K. Surface heterogeneity of zirconia-supported V_2O_5 catalysts. The link between structure and catalytic properties in oxidative dehydrogenation of propane. *Langmuir* **1999**, *15*, 5733–5741. [CrossRef]
35. Deo, G.; Wachs, I.E. Reactivity of supported vanadium oxide catalysts: The partial oxidation of methanol. *J. Catal.* **1994**, *146*, 323–334. [CrossRef]
36. Ding, J.F.; Qin, Z.F.; Li, X.K.; Wang, G.F.; Wang, J.G. Coupling dehydrogenation of isobutane in the presence of carbon dioxide over chromium oxide supported on active carbon. *Chin. Chem. Lett.* **2008**, *19*, 1059–1062. [CrossRef]

37. Gascón, J.; Téllez, C.; Herguido, J.; Menéndez, M. Propane dehydrogenation over a Cr_2O_3/Al_2O_3 catalyst: Transient kinetic modeling of propene and coke formation. *Appl. Catal. A* **2003**, *248*, 105–116. [CrossRef]
38. Shimada, H.; Akazawa, T.; Ikenaga, N.; Suzuki, T. Dehydrogenation of isobutane to isobutene with iron-loaded activated carbon catalyst. *Appl. Catal. A* **1998**, *168*, 243–250. [CrossRef]